

The Surface Parameters of a Natural Biosorbent: Giant Reed System

Hind Khalil ^{1,*} , Fatima-Ezzahra Maarouf ¹, Mariam Khalil ¹, Sanaa Saoiabi ¹, Mhamed Hmamou ¹, Khalil Azzaoui ², Ahmed Saoiabi ¹, Bouchaib Ammary ¹

¹ Laboratory of applied chemistry of Materials(LCAM), Faculty of Sciences, Mohammed V University in Rabat, Morocco

² LCAE-URAC18, COST, Department of Chemistry, Faculty of Sciences, Mohamed 1st University, P.O. Box 717, Oujda 60000, Morocco

* Correspondence: hindkhalil8@gmail.com (H.K.);

Received: 26.02.2022; Accepted: 29.03.2022; Published: 31.05.2022

Abstract: The surface layer parameters for bark–sodium nitrate solution systems were presented. The surface charge, the biosorption of proton, hydroxyl as a function of contact time, the ionic strength, the pH (initial and final) of the suspension medium-system, and the sorbent systems' concentration were presented. Through the use of pH variation resulting from protonation/deprotonation of the surface hydroxy groups ($\overline{>SOH}$), the isoelectric point and the point of zero charges were determined. The surface charge (Q) of the electrical double layer was calculated. The ionization and complexation reactions were suggested to result in $\overline{>(MOH,Cl^-)}$, $\overline{(>MOH_2^+,Cl^-)}$ and $\overline{(>MOH,Na^+)}$ surface complexes.

Keywords: *Arundo donax* L; isoelectric point; PZC; surface property; surface charge and biosorption.

© 2022 by the authors. This article is an open-access article distributed under the terms and conditions of the Creative Commons Attribution (CC BY) license (<https://creativecommons.org/licenses/by/4.0/>).

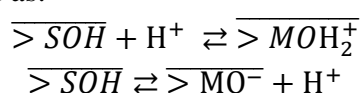
1. Introduction

The dispersion of suspension particles in an aqueous medium is combined with a surface charge (Q). This surface charge is a consequence of the ionization of acidic and basic functional groups ($\overline{>SOH}$). The dissociation of an acidic (basic) functional group results in a negatively (positively) charged surface. The net Q particle is then a function of the relative strengths of ($\overline{>SOH}$) and of the suspension pH [1,2].

In general, *Arundo donax* L. (giant reed) contains high organic and inorganic materials. The inorganic fraction is composed of calcium, magnesium, and potassium, while the organic part is reported to be lignocellulose. Lignocellulose is made up of cellulose (45-50%), hemicelluloses (35-40%), and lignin (20-24%) [3-8].

Due to its physiological characteristics and phytoremediation properties, the giant reed is used as a trace element bio-accumulator of toxic chemicals from contaminated soils. This plant is efficiently used to decontaminate polluted soils with toxic elements such as cadmium, lead, and arsenic [9-13].

Hydrated biosorbents form, in contact with water medium, a monolayer of amphoteric surface hydroxyl groups. Depending on the suspension pH, these groups ($\overline{>SOH}$) may be protonated or deprotonated, resulting in electrical surface charges (Q) [14,15]. To simplify, these processes can be described as:



The on-lined species referred to the hydrated solid phase.

The surface charge is then resulting from the dissociation of acidic/basic functional groups ($\overline{>SOH}$) of the particle surface. As a result, the net surface charge of a suspension particle is a function of the pH of the suspension medium and the relative dissociation of various $\overline{>SOH}$ functional groups. As discussed previously, ions are reorganized at the solid/liquid interface in order to keep electroneutrality [14].

The solid particles' charge and potential are generated from the dissociation of functionalized surface groups. As these groups are successively protonated/deprotonated with changes in pH, "Q" progressively changes from the charged surface up to the bulk liquid, forming an electrical double layer. This layer is composed of a compact layer (near the solid surface) and a diffuse layer that gives rise to the term electrical double layer. As the ionic strength increases, the counter-ions concentration increases and results in a continuous decrease in surface potential and a contract due to the repulsion of the functional groups.

The point of zero charge and Isoelectric point (IEP) is very important parameters for understanding the sorption mechanism as a function of the acidity of the suspension medium [16]. The accurate electrical neutrality of the suspension particle in equilibrium with an electrolyte system is then expressed in terms of its PZC. Also, it is reported that IEP as PZC of the particle suspensions corresponds to a pH value where these particles exhibit zero electrophoretic mobility [17,18].

In the absence of specific adsorption of ions, the variable-charge surface (Q), which involves protolytic reactions resulting from H^+ and OH^- sorption are found to undergo any changes with contact time or mass sorbent at $IEP=pH$. The change in the sing of surface charge with solution pH will be reflected as $\Delta pH=0$ and $Q=0$, for PZC [19].

As discussed previously, the accurate electrical neutrality of the suspension particle in equilibrium with an electrolyte system is expressed in terms of zero point of charge.

This point is representative of the internal and external surface charge, while the isoelectric point corresponds only to the external surface charge. The identical value of PZC and IEP is found to be due to a more homogeneous distribution of the surface charges and no adsorption of other ions than the proton and hydroxyl anion [1,20,21].

For this purpose, the point of zero charge and isoelectric point are determined by the kinetic-potentiometric method.

Previous investigation has shown that tree bark has a high capacity to remove organic pollutants from wastewater. But, then, more information is still required to better understand the adsorption behavior of organic and inorganic water contaminants [22-24].

The purposes of the study were to define the factors that control a biosorbent (bark), such as pH, adsorbent dose (m), contact time (t), and additive salt or ionic strength (μ).

At the isoelectric point, the surface charge properties are not affected by sorbent amount (m) or contact time (t) and the proton intake/release. As a result, the variations of pH against "t" carried out over a wide range of initial H^+ or OH^- concentrations make it possible to define the sorbent IEP. Indeed, this point corresponds to a stable pH suspension and is then coupled to the intersection point of $\Delta pH=f$ (pH) variations achieved at different "t". For this purpose, the surface chemistry of natural fibers of lingo cellulosic materials is examined as a function of several physico-chemical parameters such as pH, "t", m, and ionic strength (μ). The sorbent materials are obtained from the stem of the giant reed.

2. Materials and Methods

2.1. Material.

Chemicals used were sodium hydroxide ($NaOH$, 99%), nitric acid (HNO_3 , 99%), hydrochloric acid (HCl , 37%), sodium chloride ($NaCl$, 99%), and sodium nitrate ($NaNO_3$, 99%). All chemicals were used without further purification. These reagents of analytical grade are purchased from Sigma Aldrich. High-quality distilled water is used for all the experiments [25].

Nitric and chlorhydric acids (0.1M) were used as the stock solutions. The ionic strength, μ , was adjusted to the value of 0.001, 0.01, and 0.1 with $NaCl$ as electrolyte salts.

2.2. Preparation of *Arundo donax* fibers.

The natural bark fibers used for surface chemistry characterization were obtained from the dried stem of giant reed. Afterward, the stems are cut into a tiny fraction and then washed and dried to remove the moisture content.

The bark fibers are bundled together, forming a fiber bundle where the vessels are practically contiguous and welded. The surface chemistry is undertaken for different parts of bark: the fiber bundles or vessels and the whole bark. Experiments are conducted to investigate the effect of initial sorbent dose on surface protonation/deprotonation.

2.3. Ionization experiments of surface sorbent.

Ionization experiments of surface sorbent were examined using the technique of protonation/deprotonation of sorbent material. This technique was carried out in the batch adsorption technique. The extent of H^+/OH^- exchange with bark was achieved by examining the effect of experimental variables such as pH, adsorbent dose (0.2, 0.8, and 1.0g/L), contact time, and ionic strength. Obtained results were applied to determine the Point of Zero Charge (PZC), Isoelectric Point (IEP), and surface charge (Q). To achieve this purpose, titrations of HNO_3 (0.05M)-sorbent systems were carried out at room temperature with $NaOH$ (0.05 M). Surface charge variations against time (t) were examined for various bark mass suspensions (0.2, 0.8, and 1.0g/L).

3. Results and Discussion

3.1. Effects of solution pH at $\mu=0$.

The adsorbent dose is an essential factor that governs the proton and hydroxyl (OH^-) anion exchange performance. This factor was studied to obtain more precise data about IEP and PZC at various sorbent concentrations.

Figure 1 shows the variation of the proton (hydroxyl) adsorption/desorption rate $\frac{dpH}{dt} = f(pH)$ for $\mu=0$, $m=0.2g/L$. Contact time values vary between 15min and 70H.

As can be seen, in an acidic solution, the sorbent hydration was governed by the protonation of \overline{SOH} at a short period (2h), followed by $\overline{SOH_2^+}$ deprotonation as "t" continues to rise at $pH < 7.3$. At pH higher than 9, the sorbent pores seem to be blocked and provided no affinity to OH^- exchange, due to the formation of negative ($\overline{SO^-}$, Na^+) groups.

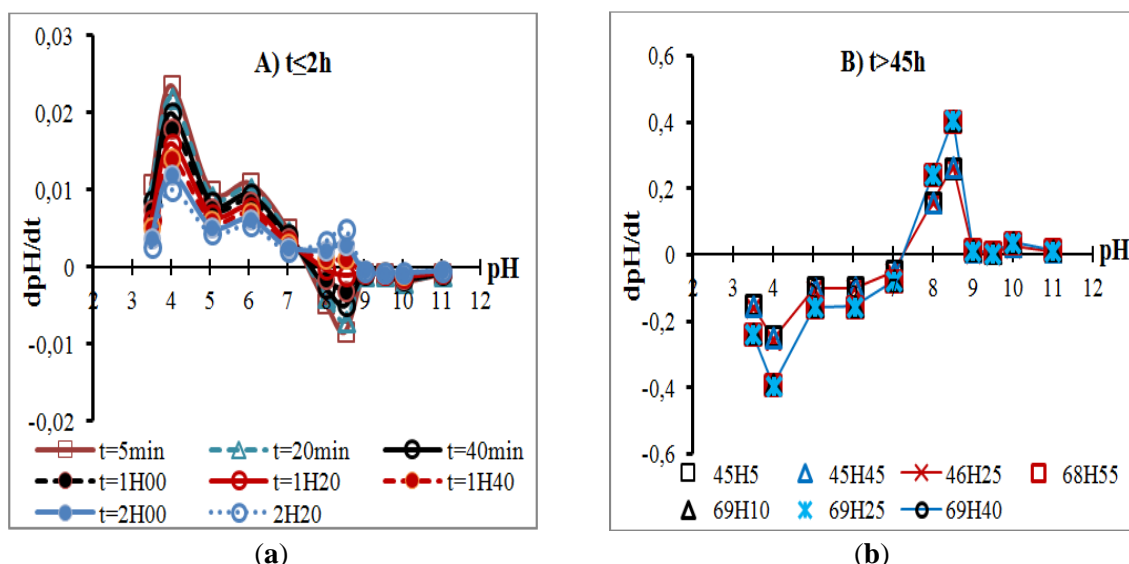


Figure 1. Variations of $\frac{dpH}{dt} = f(pH)$ obtained for whole bark at $\mu=0$, $m=0.2g/L$, (a) $t \leq 2h$; (b) $45h \leq t \leq 69h40$.

The isoelectric point is the pH value at which the effect of contact time ("t") on the pH-dependent charge was zero and was combined with the intersection point of $\frac{dpH}{dt} = f(pH)$ curves. The maximal rate of H^+ exchange was observed at a pH value of around 4. The point of zero charges was coupled to a steady pH point that was associated with a significant change of $\frac{dpH}{dt} = f(pH)$ function. In no adsorption of electrolyte ions, the rate change of pH was shown to converge to zero at a pH value corresponding to the PZC and IEP of the suspension material [16, 26].

Generally, the PZC varied in response to the adsorption of indifferent ions. Hence, adsorption of electrolyte cation on a positively (negatively) charged surface resulted in a decrease (increase) in the isoelectric point and an increase (decrease) in the point of zero charges. Adsorption of anions showed the opposite effect. As a consequence, the difference (PZC-IEP) was, among other things, a measure of the surface charge distribution of porous sorbents. Values close to zero correspond to a more homogeneous distribution of the surface charges. Values greater than zero are associated with more negatively charged externally than internal particle surfaces or just with positively internal sorbent surfaces [27].

Furthermore, examination of obtained results revealed that $\frac{dpH}{dt} = f(pH)$ graphs cross the x-axis with a sign change at the point $pH=7.3$. This x-intercept occurs when the rate ($\frac{\Delta pH}{\Delta t}$) is equal to zero. Taking into account that the isoelectric point was associated with a common point of pH versus "t" curves, the bark suspension involved surface groups characterized, in all the cases, by IEP equal to 7.3 ± 0.1 . Also, the PZC shifts from 7.5 at 20min to 8.0 at 80 min and becomes more stable and equal to 7.3 for "t" higher than 48 hours.

For such a case, the differences in the values of PZC and IEP with contact time, which resulted from the sorption of background electrolyte ion, would also be dependent on ionic strength [19,27].

Values obtained for ΔpH as a function of pH in no background electrolyte were depicted for $m=0.8g/L$ in Figure 2 for all sorbent fractions.

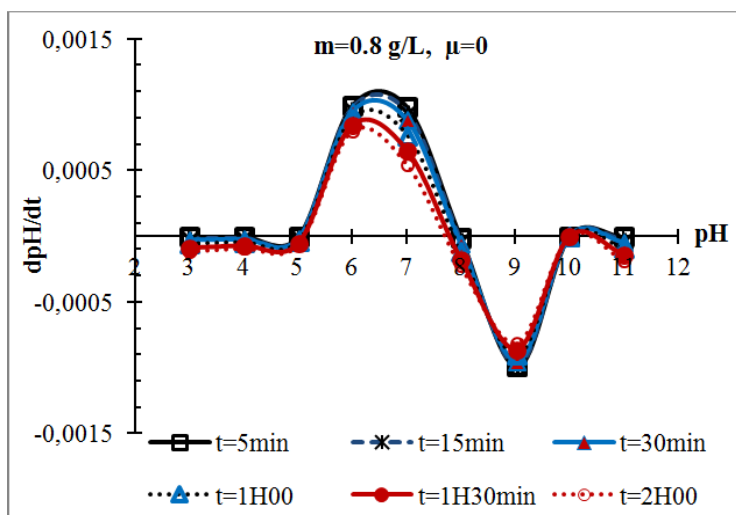


Figure 2. Variations of $\frac{dpH}{dt}=f(pH)$ obtained for whole bark at $m=0.8g/L$ and $\mu=0$.

A similar affinity in protonation-deprotonation behaviors of sorbent was obtained under various periods. In acidic solution ($pH < 5$), the suspension medium was of a buffer character due to comparable concentrations of $>SOH$ and $>SOH_2^+$. As the pH continued to rise, the exchange rate of H^+/OH^- rapidly increased and reached maxima at pH around 6 and 9. Also, started PZC occurred at $pH=7.9\pm 0.1$ and decreased to $pH=7.7\pm 0.1$ for a contact time of 2 hours. This shift of PZC with time towards lower values of pH is attributed to slight nitrate anion release. The isoelectric point was obtained at a pH value of 8.5 ± 0.1 . This single IEP value resulted from the stability and the homogeneity in the composition of the active sites.

To compare sorption ability of different bark fractions, surface characterizations were carried out for a matrix composed mainly of the outer cuticle (**Figure 3**).

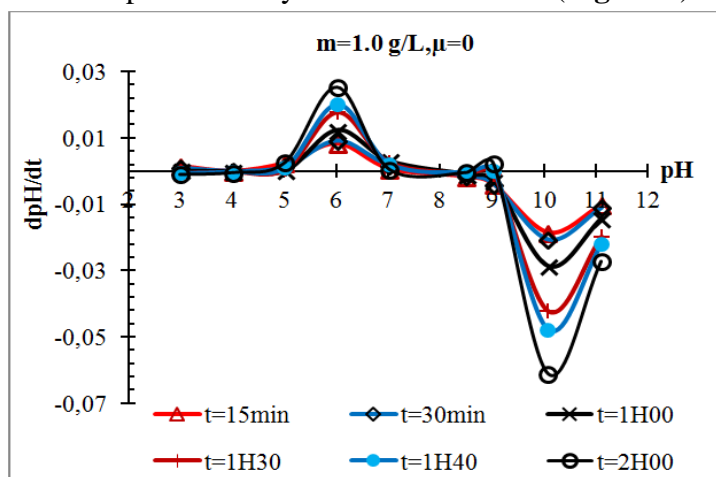


Figure 3. Variations of $\frac{dpH}{dt}=f(pH)$ obtained for fiber bundle of bark for $m=1.0g/L$ and $\mu=0$.

As can be seen from Figure 3, the fiber bundle biosorbent plays a significant role in buffering effect in acidic solution at $pH < 5$. The ability of the suspension medium to resist pH variations was due to either adsorbing or desorbing H^+ protons attached to the sorbent surface $>SOH_{1+n}^{n+}$ ($n=0$ or 1). The effect of pH controls the nature and extent of ionization of the surface groups. At lower $pH < 5$, the dissociation of $>SOH_2^+$ would be inhibited owing to the buffer property of $>SOH_{1+n}^{n+}$ ($n=0$ and $+1$) system. While due to available active sites ($>SOH$) under pH around 6, the rate formation of $>SOH_2^+$ was increased with the increase

for pH value from 5 to 6. In alkaline conditions (pH>9) there is the formation of \overline{SOH} according to the following deprotonation process:



Moreover, the x-intercepts located between pH 7.0 and 7.6, were attributed to PZC, while the overtop occurring at pH=8.5 corresponded to IEP. This well-defined isoelectric point was coupled to slight specific sorption of nitrate anion [29].

Also, values of IEP greater than those of PZC were suggested to be associated with more positively charged external particles or more negatively charged internal particles. The lower IEP value (7.3) reported for 0.2g/L suspension was due to significant internal Na^+ adsorption. The increase in the point of zero charge sometimes occurring, in this case, was suggested to be associated with surface hydration.

3.2. Effects of solution pH at $\mu = 0.05$.

To support the interpretation of experimental data obtained for $m=0.2g/L$ and to better highlight the impact of ionic strength, the results relating to sodium nitrate at $\mu=0.05$ were presented in Figure 4.

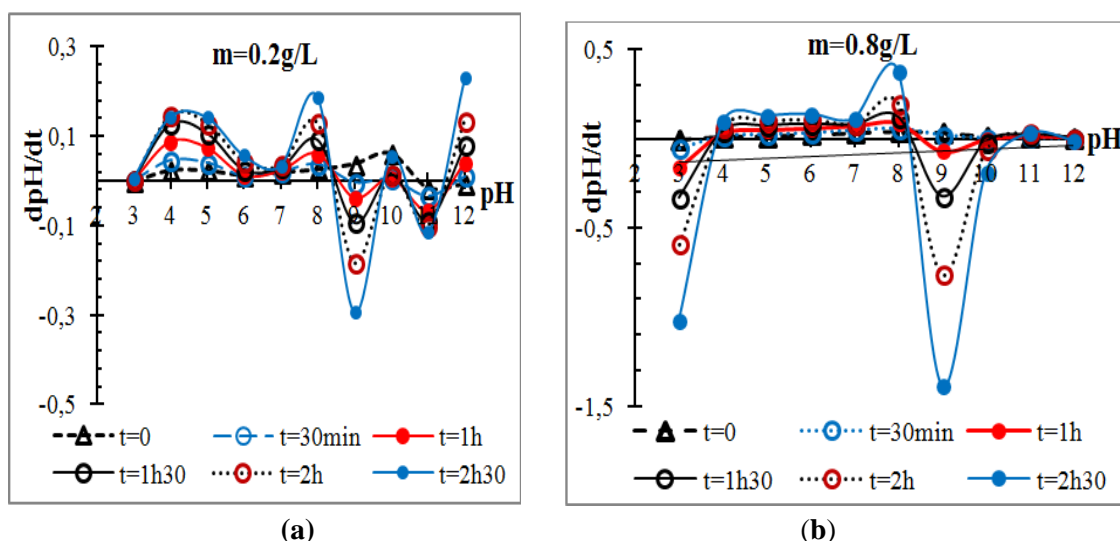


Figure 4. Variations of $\frac{dpH}{dt}=f(pH)$ obtained for whole bark at $\mu=0.05$ for (a) $m=0.2$ and (b) $0.8g/L$.

It is important to note that the solid surface was protected by columbic forces in the presence of electrolyte ions. In no sorption of these ions, columbic forces disappeared, and the ionic strength of the solution had any effect on the total surface charge. The PZC corresponding to both no net surface charge and ΔpH sign change was moreover correlated to the external pH effect [30]. From obtained results, the no effect of contact time occurred at $pH=8.3\pm 0.1$. This cross-link associated with the IEP value was also equal to PZC exhibited at (b) $0.8g/L$ suspension. The lower sorbent concentration of (a) $0.2g/L$ was more sensitive toward contamination by Na^+ and this caused a shift in the PZC to unstable higher pH values. Hence, PZC achieved in this condition was varying from 8.8 to 8.4 as the contact time increased from 0.5 to 2.5 hours. In such cases, the positive adsorption of H^+ ($\Delta pH > 0$) from solutions where $pH < PZC$ was coupled with sodium ion insertion. Oppositely, the sorption of nitrate or chloride anions results in negative adsorption of H^+ ($\Delta pH < 0$). As shown below, the reaction involved in these conditions must be considered an ionic insertion or exchange reaction.

Accordingly, data obtained in all explored suspension media showed that the isoelectric point value was equal to 8.3 ± 0.1 . The slight sorption of Na^+ or Cl^- ions resulted in PZC values ranging, respectively, from 8.3 to 8.5 and 7.0 to 7.8.

3.3. Variations of $\Delta pH=f(t)$.

The adsorption/desorption of the proton ion by barks was studied at various time intervals ($\leq 2.5h$) at $\mu=0$ and a concentration of 0.2 g/L. Figure 5 illustrated the variations of $\Delta pH= f(t)$ relative to $m=0.2$ g/L.

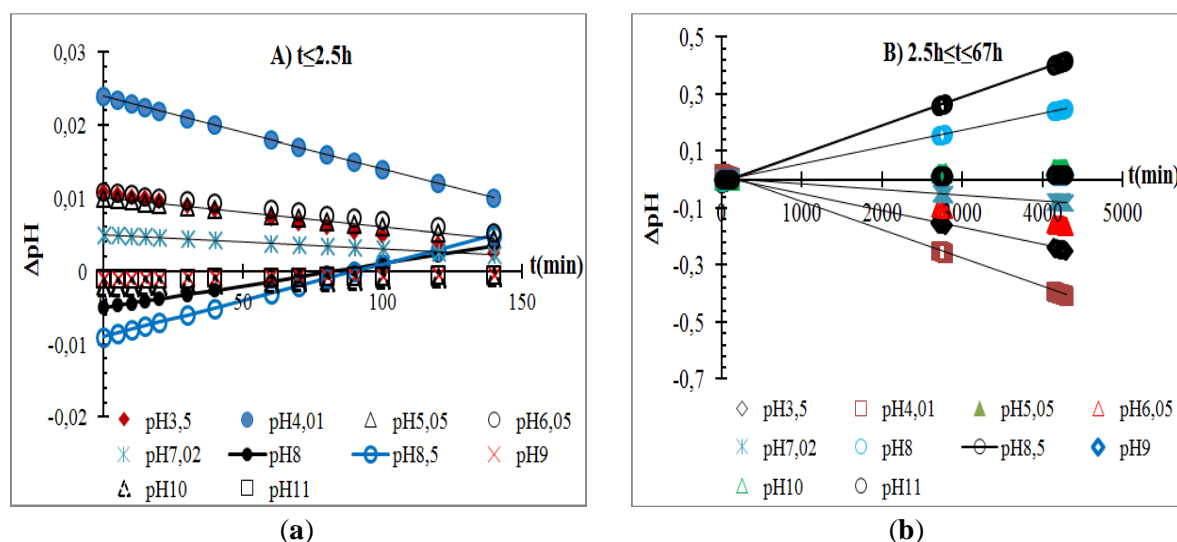


Figure 5. Variations of $\Delta pH=f(t)$ obtained for $m=0.2$ g/L at $\mu=0$ for (a) $t \leq 2.5h$ and (b) $2.5h \leq t \leq 67h$.

Plots of the surface deprotonation/dehydroxylation as a function of the pH in the absence of background electrolyte were depicted in Figure 5.

The fast proton release occurred at the lowest pH value and after that, continued at a slower rate and finally reached a stationary state at pH around 7. Then, a rapid H^+ uptake rose at pH range 8.0-8.5, followed by slight sorption at $pH \geq 9.0$, in all explored conditions. The IEP corresponding to the x-junction occurred at an average pH value of 8.3 ± 0.1 . As pH increased over pH 9, the sorbent system showed a buffering behavior. For contact duration higher than 2.5h (Figure.5B), pH continued to vary linearly with "t". The maximal $|\Delta pH|$ observed at pH values of 4.0 and 8.5 were related to extreme protonation deprotonation of $>SOH$ and $>SOH_2^+$ active sorbent groups.

3.4. Surface charge of bark.

A complementary method is used to examine the surface chemistry of barks. This is achieved from the variations of surface charge (Q) with dispersion pH, according to:

$$Q = \frac{FC\Delta V}{m} \text{ (coulomb/g)}$$

F is the faraday constant, C is the concentration of titrating acid/base, ΔV is the difference in the volume of acid used for establishing the same pH in dispersion and blank solution, and m (g/L) is the dispersion concentration of the bark particles [31].

For this purpose, the point of zero charge and isoelectric point were determined by kinetic- potentiometric method.

3.4.1. pH-dependent surface charge in NaCl electrolyte.

The pH-dependence of surface charge of bark suspensions was determined at $\mu=0.1$, 0.01, and 0.001 and for contact time (t) varying from 0.5 to 72 hours. Figure 6 showed the variations for Q against f(pH) at m= 0.2g/L and various durations.

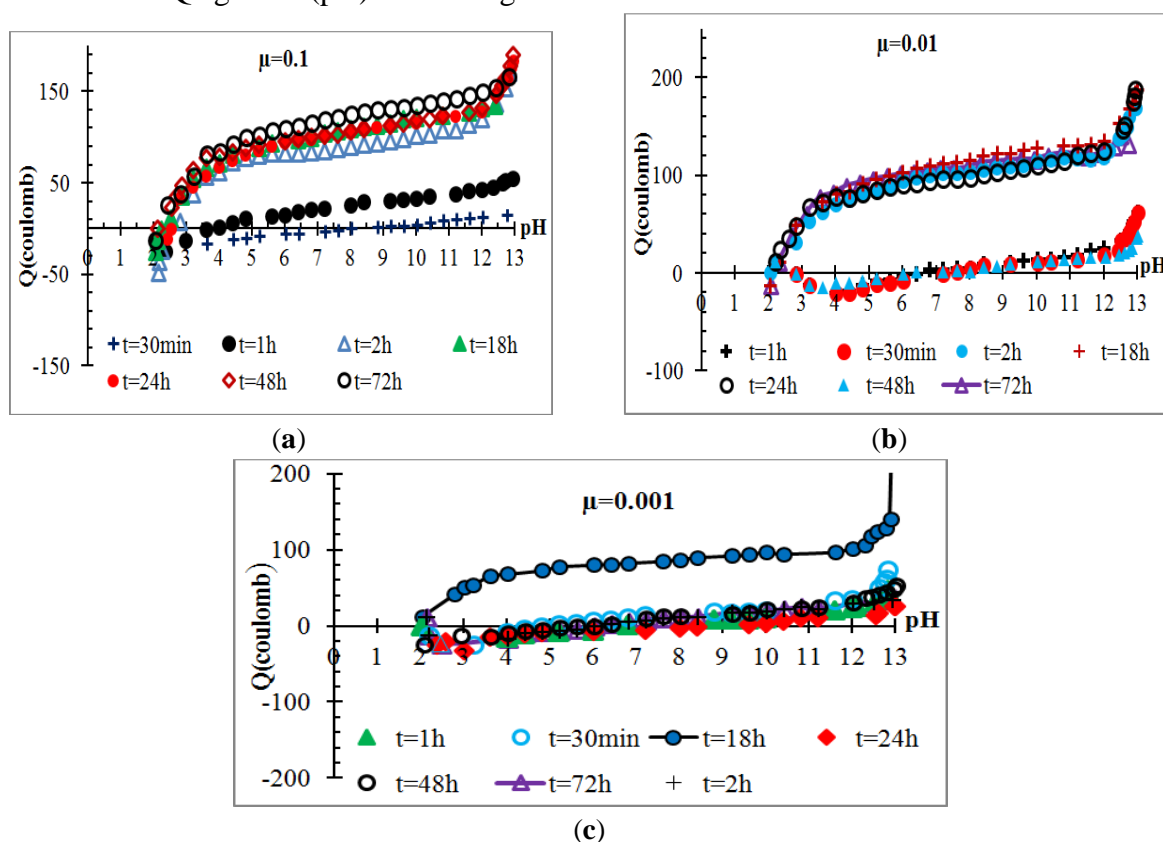
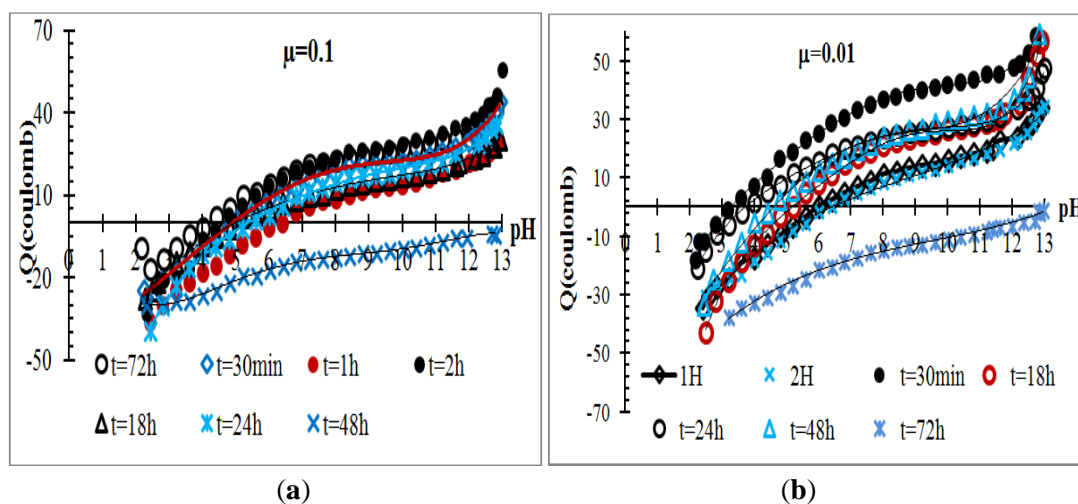
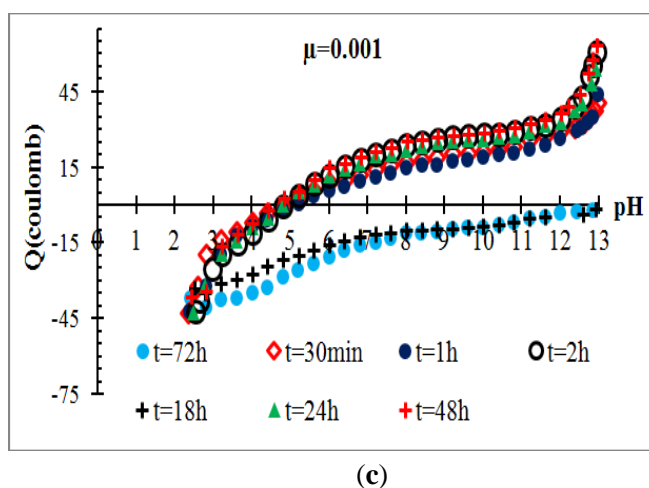


Figure 6. Variations of $Q=f(pH)$ for 0,2g/L bark suspension in $NaCl$ (a) $\mu =0.1$; (b) 0.01 and (c) 0.001M for $0.5h \leq t \leq 72h$.

As shown, the bark surface developed a "Q" charge following Na^+ and Cl^- insertions. Permanent charged sites were involved essentially in no H^+/OH^- exchange reactions, mainly for pH ranging from 4 to 11. An increase in solution pH led to an increase in the concentration of the sodium surface complexes. The neutral sorbent surface was prevailing over the pH range explored at $\mu=0.001$. Excluding results obtained for 0.001M $NaCl$ at t=18h, the zero value of Q associated with x-intercepts was often achieved at $pH \approx 2.5 \pm 0.3$.





(c)

Figure 7. Variations Q in function of pH obtained for braks at $m=0.8\text{g/l}$ in NaCl 0.1 (a), 0.01(b), 0.001M (c) at $0.5\text{h} \leq t \leq 72\text{h}$.

A maximal Q value ranging from 100 to 150 coulombs was reached at pH around 12, in all explored conditions. The slow uptake rate of Na^+ that was slightly pH-dependent was essentially owing to the slow diffusion into the sorbent pores.

The curves in Figure 7 show the variations Q in the function of pH obtained for barks at $m=0.8\text{g/L}$, $\mu = 0.001, 0.01,$ and 0.1 NaCl . The similar variations of Q against pH with a fast rise in acidic medium and a plateau between pH 7 and 11.5 were respectively due to the ionic surface exchange process ($\text{pH}<7$) and Na^+ inclusion. This inclusion which was occurring at alkaline pH is due to the interaction of sodium ions with >SOH surface groups rather than with >SOH_2^+ groups that are predominating in acidic solution.

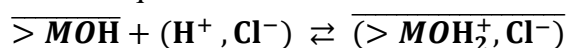
These surface reactions are:



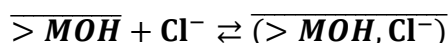
The maximum Q value of 45 coulombs which was lesser than that of 0.2g/L suspension, was achieved in all μ conditions. The minimal time required to reach this optimal charge ranged between 0.5 and 2 hours. The pH of zero charge decreased as the sorption of Na^+ increased. Indeed, while the pH of zero Q value was around 5 at $\mu=0.001$, it ranged from 3.2 to 6.8 for $\mu = 0.01$ and from 4.4 to 6.4 for $\mu = 0.1$.

Furthermore, the negative Q value, which decreases with an increase in pH is, resulting from a procedure similar to H^+ exchange reaction[27].

Taking into account that >SOH_2^+ groups are predominating in acidic solution, the Cl-sorption reaction agrees with the equation:



At alkaline pH, the slight retention of chloride anions is due to the diffusion phenomenon, which is associated with the following process:



3.4.2. Effect of contact time on zero charge.

A. Effect of ionic strength

To better highlight the impact of ionic strength and contact time on a surface charge, the pH of zero Q, $pH_{Q=0}$, was examined for $\mu=0.001$, 0.01, and $\mu =0.1$ at $t \leq 72h$. The experimental data obtained for $m=0.8g/L$ were rearranged and presented in Figure 8.

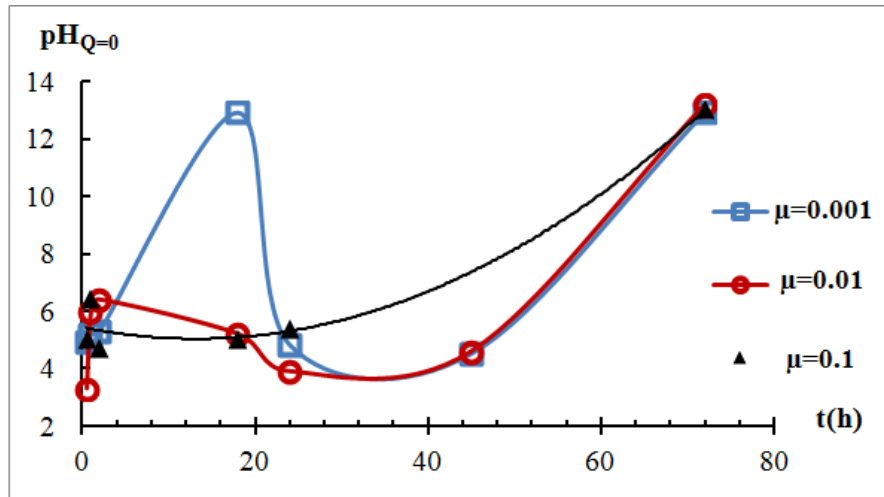


Figure 8. Variations of zero Q in function of contact time obtained for barks at $m=0.8g/L$ in $\mu = 0.1, 0.01,$ and $0.001M$.

Examination of this figure shows that the effect of ionic strength generally resulted in an important difference of $pH_{Q=0}$ during the first eighteen hours. Thereafter, due to the high stability of the bark suspensions, comparable values of $pH_{Q=0}$ were obtained at the same contact period.

B. Effect of contact time at constant pH

The variations of the surface charge at a given pH and various contact times were depicted in Figure 9, for $m=8.0g/L$ and at $\mu =0.01$ and $\mu = 0.1$.

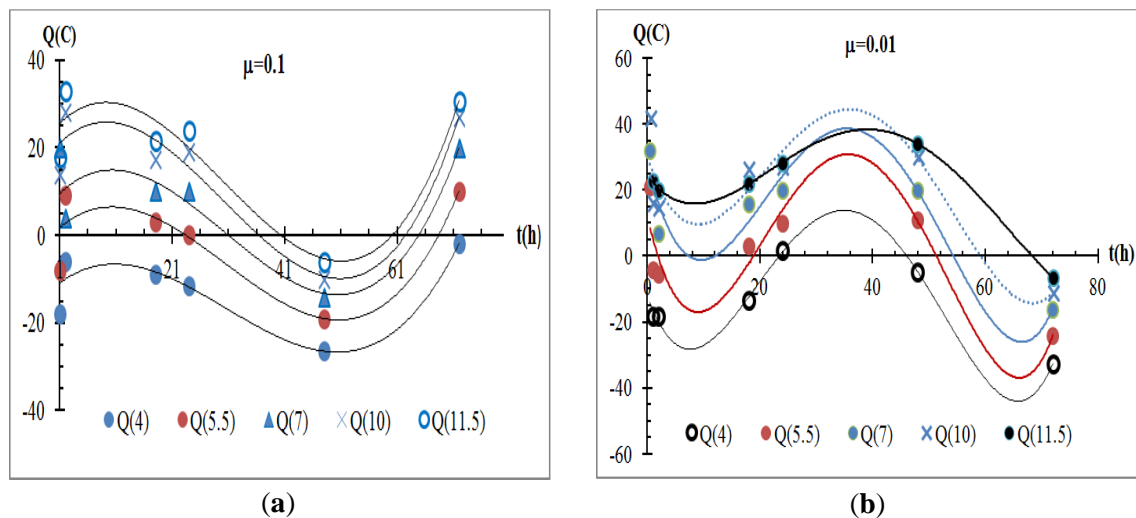


Figure 9. Variations of Q_C at a given pH against contact time, for $m=0.8g/L$ at (a) $\mu = 0.1$ and (b) 0.01 .

Experimental results showed Q varying sinusoidally with time. These variations characterized by different durations (T_i) of zero surface charge, were achieved in opposite

phases. The contact time and the solution pH were the main factors affecting H^+ adsorption/release. Subsequently, the choice of "t" parameter was crucial for the efficient design of this adsorption process that may be suggested for treating constant pH systems, such as natural waters.

The duration of Ti as a function of pH and electrolyte concentration as illustrated in Figure 10.

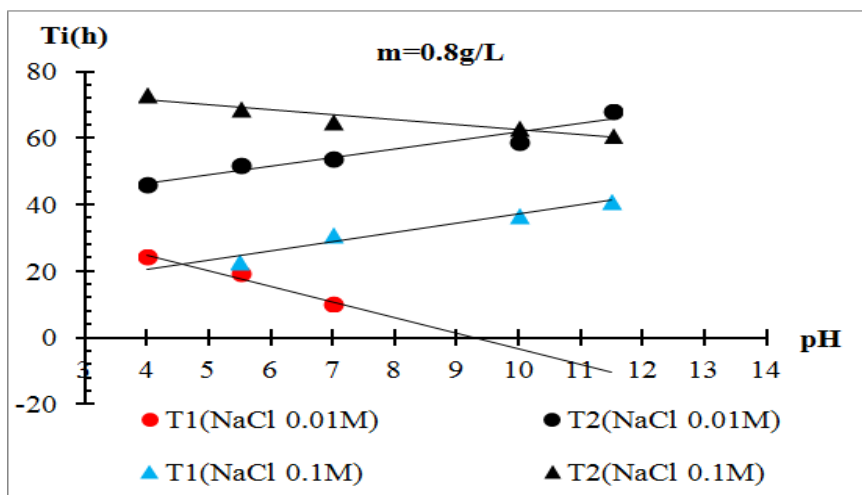


Figure 10. Variations of the adsorption period of Na^+ and Cl^- ions as a function of the pH for $m=0.8g/L$ and $\mu_1=0.01$ and $\mu_2=0.1$.

The points of no-surface charge were significantly dependent on Na^+ and Cl^- concentrations. At the same Na^+ or Cl^- concentration, opposite pH effects were found for adsorption time T1 and T2. Although, μ should not have any effect and resulted in similar $Ti=f(pH)$ variations at $\mu=0.01$ and 0.1 .

It seems important to note that the zero charge was none other than the neutral complex ($>MOH_2^+, Cl^-$) Whereas the positive and negative Q corresponded respectively to ($>MOH, Na^+$) and ($>(MOH, Cl^-)$) species. As found, the charged complexes often appeared spontaneously in explored conditions, whereas ($>MOH_2^+, Cl^-$) formation was faster at lower pH.

4. Conclusions

In this study, a procedure has been developed for sorbent's surface chemistry, which corresponds to bark materials. The solution pH, adsorbent dosage, contact time, and electrolyte salt greatly impacted sorbent surface properties. The kinetic of H^+ and OH^- the exchange was used to define the IEP and PZC of the biomaterial. In this case, results were obtained through examination of different derivative plots of $\frac{\Delta pH}{\Delta t} = f(pH)$.

These plots provide a single intersection point at $pH=IEP=8.4\pm 0.1$. This point was not affected by sorbent amount (m) or contact time (t); nevertheless, PZC varied between 7.0 and 7.7 due to the sorption of electrolyte ions (Na^+ , Cl^-). Furthermore, the plots of ΔpH against contact time (t) provided clear intersection points at an IEP value of 8.3 ± 0.1 .

The variable charged biosorbent adopted a negative surface charge at low pH and a positive surface charge at high pH. Surface complexes have been developed due to the insertion of electrolyte ions, which resulted in ($>(MOH, Cl^-)$), ($>MOH_2^+, Cl^-$) and ($>MOH, Na^+$) species. Sinusoidal variations of Q versus time were obtained at constant acidities and led to

two zero charge values for a given pH. A zero charge was obtained at two periods that were varying with "t" in opposite directions

Funding

This research received no external funding.

Acknowledgments

The authors would like to thank Mohammed V University in Rabat for executing this research work in the Applied Chemistry Laboratory Materials. It has provided us with all the necessary chemical products and measurement equipment.

Conflicts of Interest

The authors declare that they have no conflict of interest.

References

1. Menéndez, J.A.; Illán-Gómez, M.J.; Lèon y Lèon, C.A.; Radovic, L.R. On the difference between the isoelectric point and the point of zero charge of carbons. *Carbon* **1995**, *33*, 1655-1659, [https://doi.org/10.1016/0008-6223\(95\)96817-R](https://doi.org/10.1016/0008-6223(95)96817-R).
2. Hmamou, M.; Maarouf, F.; Ammary, B.; Bellaouchou, A. adsorption of citric acid on iron (III) hydroxide: mechanisms and stability constants of surface complexes. *RASĀYAN J. Chem.* **2021**, *14*, 1255-1264, <http://dx.doi.org/10.31788/RJC.2021.1426231>.
3. Suárez, L.; Castellano, J.; Romero, F.; Marrero, M.D.; Benítez, A.N.; Ortega, Z. Environmental Hazards of Giant Reed (*Arundo donax* L.) in the Macaronesia Region and Its Characterisation as a Potential Source for the Production of Natural Fibre Composites. *Polymers* **2021**, *13*, 2101, <https://doi.org/10.3390/polym13132101>.
4. Antal, G. Giant reed (*Arundo donax* L.) from ornamental plant to dedicated bioenergy species: review of economic prospects of biomass production and utilization. *Int. J. of Horticultural Science* **2018**, *24*, 39-46, <https://doi.org/10.31421/IJHS/24/1-2./1545>.
5. Di Fidio, N.; Fulignati, S.; De Bari, I.; Antonetti, C.; Raspolli Galletti, A.M. Optimisation of glucose and levulinic acid production from the cellulose fraction of giant reed (*Arundo donax* L.) performed in the presence of ferric chloride under microwave heating. *Bioresource Technology* **2020**, *313*, 123650, <https://doi.org/10.1016/j.biortech.2020.123650>.
6. Perduca, M.; Bovi, M.; Destefanis, L.; Nadali, D.; Fin, L.; Parolini, F.; Sorio, D.; Carrizo, M.E.; Monaco, H.L. Structure and properties of the giant reed (*Arundo donax*) lectin (ADL). *Glycobiology* **2021**, *31*, 1543–1556, <https://doi.org/10.1093/glycob/cwab059>.
7. Bessa, W.; Trache, D.; Derradji, M.; Ambar, H.; Tarchoun, A.F.; Benziane, M.; Guedouar, B. Characterization of raw and treated *Arundo donax* L. cellulosic fibers and their effect on the curing kinetics of bisphenol A-based benzoxazine. *Inter. J. Bio. Macro* **2020**, *164*, 2931–2943, <https://doi.org/10.1016/j.ijbiomac.2020.08.179>.
8. Chen, Z.; Jiang, D.; Zhang, T.; Lei, T.; Zhang, H.; Yang, J.; Shui, X.; Li, F.; Zhang, Y.; Zhang, Q. Comparison of three ionic liquids pretreatment of *Arundo donax* L. For enhanced photo-fermentative hydrogen production. *Bioresource Technology* **2021**, *343*, 126088, <https://doi.org/10.1016/j.biortech.2021.126088>.
9. Alshaal, T.; Elhawati, N.; Domokos-Szabolcsy, É.; Kátai, J.; Márton, L.; Czakó, M.; El-Ramady, H.; Fári, M.G. Giant Reed (*Arundo donax* L.): A Green Technology for Clean Environment. In: *Phytoremediation: Management of Environmental Contaminants* **2015**, *1*, 3-20, https://doi.org/10.1007/978-3-319-10395-2_1.
10. Zhang, D.; Jiang, Q.W.; Liang, D.Y.; Huang, S.; Liao, J. The Potential Application of Giant Reed (*Arundo donax*) in Ecological Remediation. *Front. Environ. Sci.* **2021**, *9*, 652367, <https://doi.org/10.3389/fenvs.2021.652367>.

11. Vasmara, C.; Cianchetta, S.; Marchetti, R.; Ceotto, E.; Galletti, S. Potassium Hydroxyde Pre-Treatment Enhances Methane Yield from Giant Reed (*Arundo donax* L.). *Energies* **2021**, *14*, 630, <https://doi.org/10.3390/en14030630>.
12. Danelli, T.; Sepulcri, A.; Masetti, G.; Colombo, F.; Sangiorgio, S.; Cassani, E.; Anelli, S.; Adani, F.; Pilu, R. *Arundo donax* L. Biomass Production in a Polluted Area: Effects of Two Harvest Timings on Heavy Metals Uptake. *Appl. Sci.* **2021**, *11*, 1147, <https://doi.org/10.3390/app11031147>.
13. Cristaldi, A.; Fiore, M.; Oliveri Conti, G.; Pulvirenti, E.; Favara, C.; Grasso, A.; Copat, C.; Ferrante, M. Phytoremediation potential of *Arundo donax* (Giant Reed) in contaminated soil by heavy metals. *Environmental Research* **2020**, *185*, 109427, <https://doi.org/10.1016/j.envres.2020.109427>.
14. Hernandez, P.B.; Ibanez, J.G.; Godinez-Ramirez, J.J.; and Almada-Calvo, F. Microscale Environmental Chemistry: Part 7. Estimation of the Point of Zero Charge (PZC) for Simple Metal Oxides by a Simplified Potentiometric Mass Titration Method. *Chem. Educator.* **2006**, *11*, 267-270, <https://doi.org/10.1333/s00897061012a>.
15. Shatla, A.S.; Landstorfer, M.; Baltruschat, H. On the Differential Capacitance and Potential of Zero Charge of Au(111) in Some Aprotic Solvents. *ChemElectroChem* **2021**, *8*, 1817–1835, <https://doi.org/10.1002/celec.202100316>.
16. Ibanez, J.G.; Hernandez-Esparza, M.; Doria-Serrano, C.; Fregoso-Infante, A.; Singh, M.M. The Point of Zero Charge of Oxides. In: *Environmental Chemistry*. 1st Ed., New York, **2008**, 70-78, https://doi.org/10.1007/978-0-387-49493-7_5.
17. Kosmulski, M. The pH dependent surface charging and points of zero charge. IX. Update. *Advances in Colloid and Interface Science* **2021**, *296*, 102519, <https://doi.org/10.1016/j.cis.2021.102519>.
18. Al-Maliky, E.A.; Gzar, H.A.; Al-Azawy, M.G. Determination of Point of Zero Charge (PZC) of Concrete Particles Adsorbents. *IOP Conf. Ser.: Mater. Sci. Eng.* **2021**, *1184*, 012004, <https://doi.org/10.1088/1757-899X/1184/1/012004>.
19. Elyahyaoui, A.; Ellouzi, K.; Al Zabadi, H.; Razzouki, B.; Bouhlassa, S.; Azzaoui, K.; Mejdoubi, E.; Hamed, O.; Jodeh, S.; Lamhamdi, A. Adsorption of Chromium (VI) on Calcium Phosphate: Mechanisms and Stability Constants of Surface Complexes. *Appl. Sci.* **2017**, *7*, 222-236, <https://doi.org/10.3390/app7030222>.
20. Bjjjou, W.; El Yahyaoui, A.; Bouhlassa, S.; El Belghiti, M.A. Determination of zero charge point of a biosorbent which origin is vegetable. *Der Pharma Chemica* **2016**, *8*, 258-261.
21. Kollannur, N.J.; Arnepalli, D.N. Methodology for Determining Point of Zero Salt Effect of Clays in Terms of Surface Charge Properties. *J. Mater. Civ. Eng.* **2019**, *31*, 04019286, [https://doi.org/10.1061/\(ASCE\)MT.1943-5533.0002947](https://doi.org/10.1061/(ASCE)MT.1943-5533.0002947).
22. Salman, M.; Rehman, R.; Farooq, U.; Tahir, A.; Mitu, L. Biosorptive Removal of Cadmium(II) and Copper(II) Using Microwave-Assisted Thiourea-Modified Sorghum bicolor Agrowaste. *Journal of Chemistry* **2020**, *11*, 8269643, <https://doi.org/10.1155/2020/8269643>.
23. Yang, T.; Xu, Y.; Huang, Q.; Sun, Y.; Liang, X.; Wang, L.; Qin, X.; Zhao, L.; Xu, Y. Adsorption characteristics and the removal mechanism of two novel Fe-Zn composite modified biochar for Cd(II) in water. *Bioresource Technology* **2021**, *333*, 125078, <https://doi.org/10.1016/j.biortech.2021.125078>.
24. Okoro, H.K.; Pandey, S.; Ogunkunle, C.O.; Ngila, C.J.; Zvinowanda, C.; Jimoh, I.; Lawal, I.A.; Orosun, M.M.; Adeniyi, A.G. Nanomaterial-based biosorbents: Adsorbent for efficient removal of selected organic pollutants from industrial wastewater. *Emerging Contaminants* **2022**, *8*, 46-58, <https://doi.org/10.1016/j.emcon.2021.12.005>.
25. Hmamou, M.; Maarouf, F.; Ammary, B.; Bellaouchou, A. Surface Complexation of Chromium (VI) on Iron (III) Hydroxide: Mechanisms and Stability Constants of Surfaces Complexes. *Indones. J. Chem.* **2021**, *21*, 679 – 689, <https://doi.org/10.22146/ijc.60634>.
26. Kozłowski, L.P. Proteome-*pI* 2.0: proteome isoelectric point database update. *Nucleic Acids Research* **2022**, *50*, 1535–1540, <https://doi.org/10.1093/nar/gkab944>.
27. Ntakirutimana, S.; Tan, W.; Wang, Y. Enhanced surface activity of activated carbon by surfactants synergism. *RSC Advances* **2019**, *9*, 26519–26531, <https://doi.org/10.1039/C9RA04521J>.
28. Janusz, W. The Electrical Double Layer Parameters for the Group 4 Metal Oxide/ Electrolyte System. *Adsorption Science & Technology* **2000**, *18*, 117-134, <https://doi.org/10.1260/0263617001493332>.
29. Cristiano, E.; Hu, Y.J.; Siegfried, M.; Kaplan, D.; Nitsche, H. A comparison of Point of Zero Charge measurement methodology. *Clays and Clay Minerals* **2011**, *59*, 107-115, <https://doi.org/10.1346/CCMN.2011.0590201>.
30. Kosmulski, M.; Mączka, E. The Isoelectric Point of an Exotic Oxide: Tellurium (IV) Oxide. *Molecules* **2021**, *26*, 3136, <https://doi.org/10.3390/molecules26113136>.

31. Maarouf, F.Z.; Saoiabi, S.; Azzaoui, K.; Chrika, C.; Khalil, H.; Elkaoui, S.; Lhmir, S.; Boubker, O.; Hammouti, B.; Jodeh, S. Statistical optimization of amorphous iron phosphate: inorganic sol- gel synthesis-sodium potential insertion. *BMC Chemistry* **2021**, *15*, 48, <https://doi.org/10.1186/s13065-021-00774-x>.